Fish and Shellfish Immunology 90 (2019) 395–403

Contents lists available at ScienceDirect

Fish and Shellfish Immunology

journal homepage: www.elsevier.com/locate/fsi

Full length article

Molecular characterization and functional activity of *Prx1* in grass carp (*Ctenopharyngodon idella*)

Denghui Zhu[a,b], Yangyang Li[a,b], Rong Huang[a], Lifei Luo[a,b], Liangming Chen[a,b], Peipei Fu[a,b], Libo He[a], Yongming Li[a], Lanjie Liao[a], Zuoyan Zhu[a], Yaping Wang[a,c,*]

[a] State Key Laboratory of Freshwater Ecology and Biotechnology, Institute of Hydrobiology, Chinese Academy of Sciences, Wuhan, 430072, China
[b] University of Chinese Academy of Sciences, Beijing, 100049, China
[c] Innovative Academy of Seed Design, Chinese Academy of Sciences, Beijing, 100101, China

ARTICLE INFO

Keywords:
Peroxiredoxin 1 (Prx1)
Immune response
Recombinant protein
Antioxidant activity
Subcellular localization

ABSTRACT

Peroxiredoxin (Prx) family are known as an important antioxidant enzyme as the first line of defense against oxidative damage, and also involved in immune responses following viral and bacterial infection. Here, a full-length Prx1 cDNA sequence (*CiPrx1*) was cloned from grass carp (*Ctenopharyngodon idella*), which was 1029 bp, including a 5′-terminal untranslated region (UTR) of 121 bp, a 3′-UTR of 272 bp, an open reading frame of 600 bp encoding 199 amino acids with molecular weight of 22.21 kDa and isoelectric point of 6.30. CiPrx1 shares 80.8–99% protein sequence similarity with Prx1 of other fishes. The conserved peroxidase catalytic center "FYPLDFTFVCPTEI" and "GEVCPA" were observed in the sequence of CiPrx1; this indicated that it was a member of 2-Cys Prx. Subcellular localization of CiPrx1 was only strongly distributed in the cytoplasm. Quantitative real-time PCR (RT-qPCR) assays revealed that *CiPrx1* mRNA was ubiquitously detected in all tested tissues, and the expression was comparatively high in liver, gill and spleen. Further, the expression of *CiPrx1* can be induced by grass carp reovirus (GCRV), lipopolysaccharide (LPS) and polyinosinic:polycytidylic acid (Poly I:C) infection in the different tissues. Moreover, the recombinant CiPrx1 (rCiPrx1) protein was found a potential antioxidant enzyme, that could inhibit DNA damage from oxidants. Altogether, our results imply that *CiPrx1* is associated with defending against virus and bacteria pathogens and oxidants in grass carp.

1. Introduction

The grass carp (*Ctenopharyngodon idella*) is one of the most important freshwater aquaculture species in China. However, hemorrhagic disease caused by grass carp reovirus (GCRV) seriously affects the grass carp cultivation industry [1–5]. GCRV is a double-stranded RNA virus belonging to the genus *Aquareovirus* (AQRV), family *Reoviridae* [6], which causes severe hemorrhagic disease with approximately 85% mortality in fingerling and yearling grass carp in China [7]. In view of this, it would have important significance to study the immune response mechanism in grass carp.

Oxidative stress imposed either directly by the virus or by the host-immune response, is a potentially important pathogenic mechanism in many virus infectious diseases [8–11]. The generation of reactive oxygen species (ROS) can be induced under various conditions of stress, including ionizing radiation, chemotherapeutic drugs and viral infections [12]. ROS are involved in various cellular processes such as proliferation, apoptosis, and inflammation [13]. However, ROS like the superoxide anion, hydrogen peroxide, and the hydroxyl radical [14], causing serious oxidative stress and leading to protein oxidation, lipid peroxidation, DNA strand break, DNA base modifications and cell death [15,16]. To defend against excessive ROS, the organisms have developed protective mechanisms, including superoxide dismutase (SOD), catalase (CAT) and many types of peroxidases (Prx) [17–19]. Prxs are known as an important antioxidant enzyme as the first line of defense against oxidative damage from excessive ROS levels [20]. Based on the number of conserved cysteine residues, the members of Prxs family can be classified into six subtypes: the typical 2-Cys type (Prx1, Prx2, Prx3 and Prx4), the atypical 2-Cys type (Prx5) and 1-Cys type (Prx6) [21]. The first member of Prxs family was discovered in yeast *Saccharomyces cerevisiae* [22]. Prxs exist ubiquitously in most species, which regulate the redox state of target proteins through peroxide-dependent oxidation and thiol-dependent reduction during catalysis via the reversible oxidation of their active site dithiol (thiol, O_2, catalytic amounts of contaminating Fe^{3+}) with a TRX-fold domain [23]. Prxs can eliminate the immune response and inflammation caused by biotic and abiotic

* Corresponding author. Institute of Hydrobiology, Chinese Academy of Sciences, Wuhan, 430072, China.
E-mail address: wangyp.ihb@gmail.com (Y. Wang).

https://doi.org/10.1016/j.fsi.2019.04.302
Received 1 January 2019; Received in revised form 26 April 2019; Accepted 28 April 2019
Available online 01 May 2019

stresses. Besides, Prxs also play important roles in cell proliferation and differentiation, protecting DNA against mutation, suppressing tumor formation and so on [24–30], [31]. Prx1 is a typical two-Cys-Prxs, which has been reported in mouse RAW264.7 cells [32], cuttlefish (*Sepiella maindroni*) [33], *Lateolabrax japonicas* [34], bumblebee *Bombus ignites* [35], *Trachinotus ovatus* [36], and the crustacean *Eurypanopeus depressus* [37].

For better understanding the functional role of Prx1, we isolated and characterized the *Prx1* gene from *C. idella* (*CiPrx1*), and determined its spatial expression. In addition, we evaluated the expression profile of *CiPrx1* following LPS, Poly I:C and GCRV challenge at different time points. The enzyme activity of recombinant CiPrx1 (rCiPrx1) protein was evaluated by mixed-function oxidase assay. The results of the present study will provide further insight for better understanding the function of *CiPrx1* in teleosts.

2. Materials and methods

2.1. Ethics statement

All animal experiments were complied with the ARRIVE guidelines and were carried out in accordance with the National Institutes of Health guide for the care and use of Laboratory animals (NIH Publications No. 8023, revised 1978). All protocols were approved by the committee of the Institute of Hydrobiology, Chinese Academy of Sciences (CAS). The reference number obtained was Y11201-1-301 (Approval date: 30 May 2016). All surgeries were performed under eugenol anesthesia (final concentration: 100 mg/L) and all efforts were made to minimize suffering.

2.2. Fish, cell line and transfection

Three-month-old healthy grass carps (weight, about 10 g; average length, 7 cm) were provided by the GuanQiao Experimental Station, Institute of Hydrobiology, Chinese Academic of Sciences, and acclimatized in aerated freshwater at 28 °C for 1 week before processing. Animals were fed with a commercial feed (Tong Wei, China) twice a day at the same conditions. For tissue distribution analysis of mRNA expression, tissues including skin, gill, intestine, liver, spleen, head kidney, middle kidney, muscle, heart and brain were collected from 5 healthy grass carp. The GCRV infection experiment was carried out as described previously [2,38] with modifications. Grass carps were injected intraperitoneally with GCRV (GD108 strain, 3.12×10^3 copy/ul,10 μl/g body weight). The control animals were injected with PBS. Five individuals were dissected and tissues including liver, spleen, head kidney and middle kidney were sampled at 0, 1, 3, 5 and 7 days post injection (dpi). For detecting the mRNA expression levels of target genes under pathogen-associated molecular patterns (PAMPs) stimulation, each fish of challenge groups was injected intraperitoneally with 200 μl LPS (L2880, Sigma, from *Escherichia coli* 055: B5, 0.5 mg/ml) or 200 μl Poly I:C (27472901, GE, 1 mg/ml) in phosphate buffered saline (PBS), respectively. And fish of the control group was injected with the same volume of PBS. At 3, 6, 12, 24, and 48 h post injection (hpi), 5 fish from each group were anaesthetized in eugenol anesthesia (final concentration: 100 mg/L), and different tissues including spleen, liver, middle kidney and head kidney were collected. All above of the tissues were homogenized in TRIzol reagent (Invitrogen, USA) for RNA extraction.

Human embryonic kidney 293T (HEK 293T) cells were cultured in high glucose Dulbecco's modified Eagle's medium (DMEM; Hyclone, USA), with 10% FBS, 100 IU/ml penicillin (Sigma, USA) and 100 mg/ml streptomycin (Sigma, USA) under a humidified condition with 5% CO_2 at 37 °C. Transfection of plasmids in HEK 293T cells was performed using Lipo6000™ Transfection Reagent (Beyotime) according to manufacturer's instructions.

Table 1
Primers used in this study.

Primers	Sequences (5′—3′)	Purpose
Prx1-5′Rout	GGACGTCGGGCTTAATTGTGTC	5′ RACE
Prx1-5′Rin	CAAACAAAGGTGAAATCCAATGG	
Prx1-3′Rout	GCAAACCTGCTCCAGACTTCAC	3′ RACE
Prx1-3′Rin	ATTGATGACAAAGGCATTCTGAGG	
Prx1-F	ATGGCAGCTGGAAAAGCACA	ORF cloning
Prx1-R	TTAGTGTTGTTTGGAGAAGTAGTCTTTG	
qPrx1-F	GCAAACCTGCTCCAGACTTCAC	qRT-PCR
qPrx1-R	CAAACAAAGGTGAAATCCAATGG	
qβ-actin-F	TCGGTATGGGACAGAAGGAC	
qβ-actin-R	GACCAGAGGCATACAGGGAC	
qS6-F	AGCGCAGCAGGCAATTACTATCT	GCRV qRT-PCR
qS6-R	ATCTGCTGGTAATGCGGAACG	

2.3. Cloning and sequencing of CiPrx1 gene

The matched fragments of *CiPrx1* were obtained by blasting the homologous Prx1 sequences of zebrafish (Accession no. NM_001013471.2) with the draft genome of grass carp [39]. 5′ and 3′ untranslated regions (UTRs) of the *CiPrx1* gene were obtained by the rapid amplification of cDNA ends (RACE) PCR according to 5′ and 3′ Full RACE Kit (TaKaRa, Japan). The coding sequence (CDS) was amplified using PCR with primers within the 5′- and 3′-UTRs. The PCR products were purified, ligated into pMD18-T vectors (TaKaRa, Japan), and transformed into competent *Escherichia coli* DH5α cells (TransGen, China). Five positive colonies were selected and sequenced by a commercial company (Tsing Ke, China). The full-length cDNA of *CiPrx1* were obtained by comparing these PCR product sequences and discarding the obtained overlapping region sequence and vector sequence. The primers used for gene cloning and sequence verification are listed in Table 1.

2.4. Sequence analysis

BLAST (https://blast.ncbi.nlm.nih.gov/Blast.cgi) was used to search for the gene sequences of other species. The nucleotide and deduced amino acid sequence were used to search for similarity using BLASTN and BLASTP at web servers of the National Center of Biotechnology Information. ORF finder (https://www.ncbi.nlm.nih.gov/orffinder/) was used to predict the location of the open reading frame (ORF). The molecular weight (MW) and the isoelectric point (pI) of the deduced amino acid sequences were calculated by ExPASy (http://web.expasy.org/compute_pi/). The signal peptide and functional domain were predicted by using software SMART (http://smart.embl-heidelberg.de/). The *CiPrx1* sequences from different organisms were downloaded from GenBank database and used for phylogenetic analysis. Multiple sequence alignments were carried out using Multiple Alignment using Fast Fourier Transform (MAFFT) (https://www.ebi.ac.uk/Tools/msa/mafft/). A phylogenetic tree was constructed was constructed based on the amino acid sequences by MEGA 5.0 software (http://www.megasoftware.net/index.html) using Neighbor-Joining (NJ) method with bootstrap test of 1000 replications. The NJ algorithm was used as the clustering method and the distances matrix calculated using the Poisson correction method [40].

2.5. Quantitative real-time PCR

The RNA extraction and cDNA synthesis were performed as a previous report [2]. All the samples of RNA were extracted according to the manufacturer instructions for TRIzol reagent. 2 μg total RNA treated with RNase-free DNase I (Promega, USA) was used for synthesizing first-strand cDNAs by ReverTra Ace kit (Toyobo, Japan) and oligo (dT) primer in 20 μl reaction solution according to manufacturer's instructions. RT-qPCR was performed using ChamQ SYBR Color qPCR Master

Table 2
Primers used in this study.

Primers	Sequences (5′—3′)	Purpose
pEGFP-Prx1-F	CGCTCGAGGTATGGCAGCTGGAAAAGCACA	Subcellular localization
pEGFP-Prx1-R	CGGGATCCGTGTTGTTTGGAGAAGTAGTCTTTG	
pGEX-Prx1-F	CGGAATTCATGGCAGCTGGAAAAGCACA	Recombinant expression
pGEX-Prx1-R	CGCTCGAGTTAGTGTTGTTTGGAGAAGTAGTCTTTG	

Mix (Vazyme Biotech, China). The RT-qPCR cycling conditions were as follows: 95 °C for 2 min, 40 cycles of 95 °C for 10 s, annealing at 62 °C for 20 s, and 72 °C for 30 s, followed by a Melt Curve was constructed. All reactions were performed in triplicate in a 96 well plate, with the mean value recorded. The relative expression of target genes was normalized to the expression of β-actin and analyzed using the comparative Ct method ($2^{-\Delta\Delta CT}$) [41]. Statistical analysis was conducted using one way ANOVA by SPASS 16.0 and a probability level of $P < 0.05$ was considered as statistically significant. All primers used for RT-qPCR are listed in Table 1.

2.6. Protein expression and purification

PCR products (see Table 2) were digested with *EcoR* I and *Xho* I, then ligated into pGEX-4T-1 vector. The recombinant plasmid was transformed into *E. coli* BL 21 (transsetta DE3) competent cells (TransGen Biotech, Beijing, China), and confirmed by sequencing. The positive plasmid was induced by Isopropyl-β-D-thiogalactoside (IPTG, at a final concentration of 1 mM) at 37 °C, 220 r/min. After 4 h of induction, the cells were harvested by centrifugation, resuspended, sonicated and then centrifuged again. The recombinant proteins were analyzed by 12% SDS-PAGE and then transferred to a polyvinylidene difluoride (PVDF) membrane (Millipore, Massachusetts, USA) using a Mini *Trans*-Blot electrophoretic transfer system (Bio-Rad, California, USA). Membranes were blocked with 5% non-fat milk (diluted with PBS containing 0.1% Tween-20) (PBST) for 2 h at room temperature and then incubated with *anti*-GST tag antibodies (diluted 1:5000 with 5% non-fat milk in PBST) for 8 h at 4 °C. After washing with PBST, the membranes were incubated with goat anti-rabbit IgG (Beyotime, Shanghai, China) (diluted 1:5000 with 5% non-fat milk in PBST) for 1 h at room temperature. The immunoblot signal was detected using an HRP-DAB Detection Kit (Tiangen, Beijing, China). The Glutathione High Capacity Magnetic Agarose Beads (Sigma, USA) was used to purify the recombinant proteins according to the manufacturer's instructions. The purified protein concentration was determined by using the BCA Protein Assay Kit (Novagen, Hilden, Germany). The gels were visualized by Comassie blue R-250 staining.

2.7. Mixed-function oxidase assay

We performed mixed-Function Oxidase (MFO) assay to investigate the antioxidant potential of CiPrx1 according to Ref. [42] with slight modifications. The MFO assay was used to determine the degree of DNA breakage caused by the ROS generated from the thiol/Fe^{3+}/O_2^- MFO system and to what extent the CiPrx1could inhibit the DNA breakage. In short, 1 μg of substrate plasmid (pEGFP-N3) was treated with freshly prepared MFO mix (10 μM $FeCl_3$ + 10 mM DTT) and varying concentrations of the rCiPrx1 fusion protein in a total reaction volume of 20 μL. The reaction mixtures were incubated at 37 °C for 1 h. After 3 h the samples were resolved on 1% agarose gel by electrophoresis at 100 V for 25 min at room temperature. The agarose gel was stained with ethidium bromide and visualized under UV light.

2.8. Fluorescence microscopy

To analyze the subcellular localization of CiPrx1, Prx1-pEGFP vector was constructed by inserting a complete ORF of the CiPrx1 into plasmid pEGFP-N3 (Clontech, USA). First, complete ORF (amplified by primers in Table 2) was amplified from grass carp cDNA and digested with *Xho*I and *Bam*HI, then inserted into the pEGFP-N3 vector digested with the same enzymes. Sequence of the resulting plasmid was verified by DNA sequencing. HEK 293T cells were seeded into 6-well plates with 1×10^6 cells per well and cultured 24 h. After that, 5 μg of plasmid constructs of Prx1-pEGFP and pEGFP-N3 (vector control) were transfected into the cells using Lipo6000™ Transfection Reagent, respectively, according to the manufacturer's instructions. At 24 h post-transfection, the cells were fixed with 4% (v/v) paraformaldehyde, permeabilized with 0.2% Triton X-100, and stained with Hoechst 33342 (Beyotime, China) [38]. The cells were observed using the UltraVIEW VOX confocal system (PerkinElmer, Fremont, CA, USA) and a 63 × oil immersion objective lens.

3. Results and discussion

3.1. Analysis of the CiPrx1 sequence and the predicted protein

The full-length cDNA sequence of *CiPrx1* from *C. idella* was obtained, which was 1029 bp, including a 5′-terminal untranslated region (UTR) of 121 bp, a 3′-UTR of 272 bp, an open reading frame of 600 bp encoding 199 amino acids with molecular weight of 22.21 kDa and isoelectric point of 6.30 (Fig. 1). The deduced amino acid sequence of *CiPrx1* was shown in Fig. 1. Structure prediction by SMART showed that the *CiPrx1* protein sequence contained two highly conserved cysteine residues, two Prx signature motifs (FYPLDFTFVCPTEI and GEVCFA). Besides, two highly conserved cysteines (Cys52 and Cys173) lay in the signature Prx motifs FYPLDFTFVCPTEI and GEVCPA were identified, respectively. SignaIP 4.1 analysis showed that *CiPrx1* was absent from the signal peptide.

Multiple alignments and amino acid sequence similarity comparison of CiPrx1 with Prx1 in other fishes and mammals, including *Danio rerio*, *Oncorhynchus kisutch*, *Oncorhynchus mykiss*, *Clupea harengus*, *Ictalurus punctatus*, *Salmo salar*, *Homo sapiens*, *Bos taurus*, *Mus musculus* and *Rattus norvegicus* were shown in Fig. 2. The CiPrx1 protein showed highly conserved in both fish and mammals, especially in the functional area. A comparison of homology revealed that the CiPrx1 shares 71.9–99% protein sequence similarity with Prx1 of other species, with it being the most similar to that of the *Cyprinus carpio* (99% sequence similarity), followed by the *Danio rerio* (92% sequence similarity) (Table 3), which revealed that CiPrx1 shared a strong homology with other fishes (80.8–99% sequence similarity), and that homology was also found among mammals (Table 3). For clarifying the molecular evolutionary relationship, a phylogenetic tree was constructed based on the deduced amino acid sequence of CiPrx1 and other genes of the TRX superfamily using the NJ method. The dendrogram showed in Fig. 3 depicted the evolutionary relationships according to the similarity of Prx1 proteins from various species, and as the results showed that Prx1could be classified into two groups: Prx1 proteins from the fishes fell into one branch; Prx1 proteins from mammals fell into another branch. Prx1 from grass carp was closely related to that of *C. carpio*, and *D.rerio*. (Fig. 3). Thus, *CiPrx1* highly evolutionarily conserved.

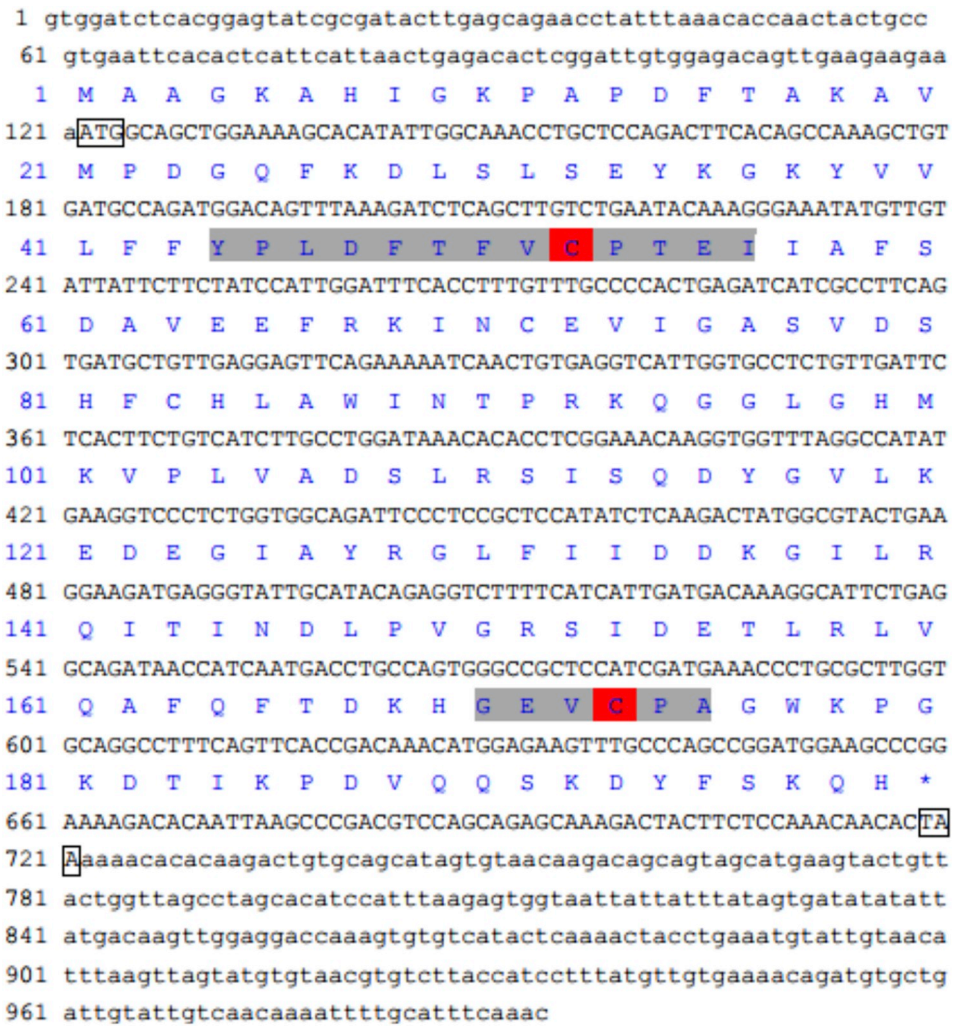

Fig. 1. Molecular characterization of *CiPrx1* cDNA. The nucleotide and deduced amino acid characteristic of *CiPrx1*. The amino acid position is marked above the figure; the nucleic acid position is marked below the figure. Boxed sequences represented initiation code (ATG) and the termination code (TAG); The Thioredoxin-like Superfamily signature is located in FYPLDFTFVCPTEI and GEVCPA; two active cysteines are red shaded. . (For interpretation of the references to colour in this figure legend, the reader is referred to the Web version of this article.).

3.2. Expression profile of CiPrx1 in different tissues

To understand the expression patterns of *CiPrx1*, 5 healthy fish tissues were sampled and subjected to RT-qPCR analysis (Fig. 4). As the results showed that *CiPrx1* was ubiquitously expressed in all tested tissues, while the expression level varied among these different tissues. In the present study, the skin was set to the calibrator, i.e., the expression level of the *CiPrx1* from the skin was defined as 1.00. The β-actin was used as an internal control. The relative high expression levels of *CiPrx1* were detected in the liver (24.57-fold), gill (6.42-fold), spleen (5.76-fold) and heart (7.27-fold), while a relative low expression pattern was detected in skin and muscle.

3.3. Analysis of CiPrx1expression following GCRV infection

Since GCRV can cause hemorrhagic symptoms in gill tissues of grass carp, the relative number of GCRV copies was expressed as the ratio of the level of the S6 segments of GCRV-II (see Table 1) expression at different time-point relative to that at 1 dpi. The β-actin was used as an internal control. As shown in Fig. 5, the number of viral copies in gill showed a gradually rising trend and the copies number significantly rising especially on the 7th day, verifying that infection had occurred (Fig. 5A). So, the large mortality of grass carp on the 7th day (data not shown) was caused by the proliferation of GCRV.

To understand whether *CiPrx1* is involved in the innate immune responses to GCRV infection, a viral challenge experiment was performed and samples were collected for RT-qPCR analysis. Upon GCRV challenge, *CiPrx1* mRNA expression levels were altered in all the detected tissues. However, the mRNA level and the time of maximum transcript level varied among them (Fig. 5B). In spleen, the maximum expression *CiPrx1* was observed on day 7(5.63-fold), then dropped back to the original level by day 5. In liver, the expression was gradually increased on the test period and the peak on day 7 (2.18-fold). Approximately similar expression patterns were recorded in middle kidney and head kidney following treatment with GCRV. The challenge of GCRV showed maximum transcript level of *CiPrx1* on day 3 in middle kidney, while the expression was highest at day 7 in head kidney.

3.4. Temporal expression of CiPrx1 mRNA challenged with PAMPs

To further investigate the physiological role of *CiPrx1,* the expression patterns of in spleen, liver, middle kidney and head kidney under conditions of bacterial infections were also detected. When grass carp individuals were treated with LPS and Poly I:C, the transcript level of *CiPrx1* in different tissues varied considerably, and the mRNA levels varied with the kind of infectious agent (Fig. 6). Poly I:C challenge

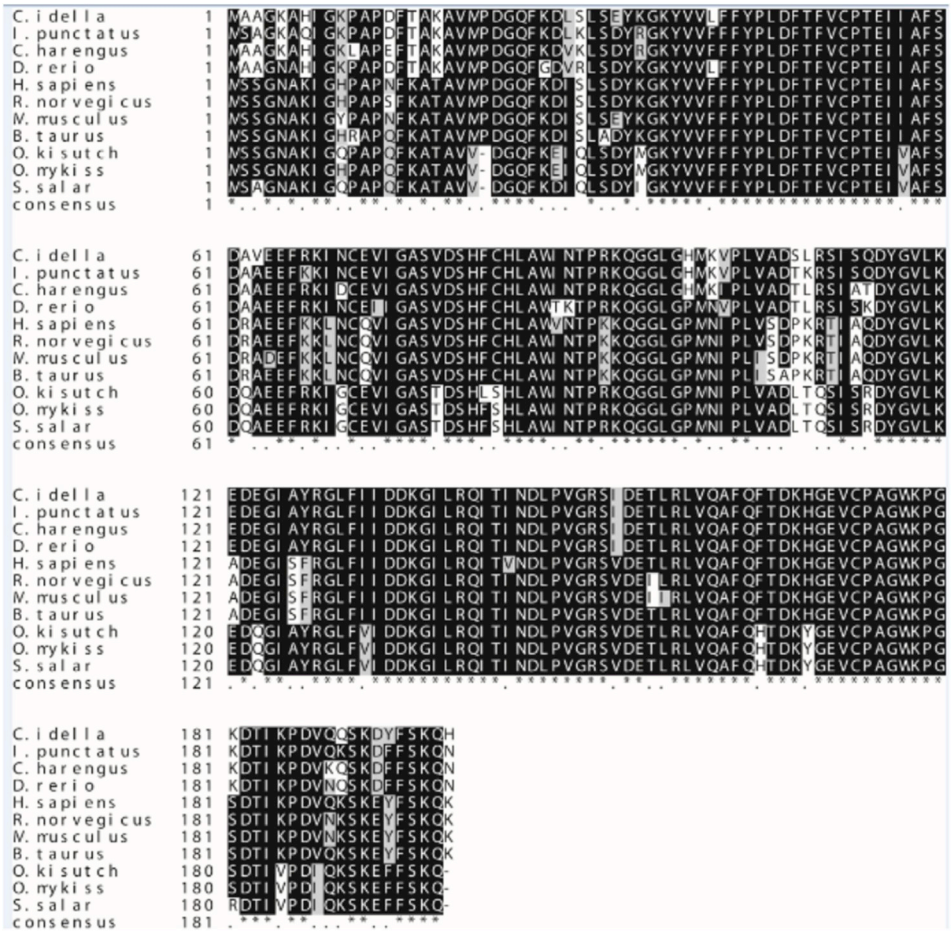

Fig. 2. Multiple alignment of *CiPrx1* with the amino acid sequences with other species; Numbers of amino acid are listed on the right side of alignments. The amino acid sequences were aligned using the ClustalW 2.1 program (http://www.ebi.ac.uk/tools/clustalw2.1). The black shade represents 100% identity, dark gray represented 80% identity. GenBank accession numbers encoding Prx1 are as follows: *Danio rerio* (NP_001013489.2), *Oncorhynchus kisutch* (XP_020309895.1), *Oncorhynchus mykiss* (XP_021412501.1), *Clupea harengus* (XP_012672962.1), *Ictalurus punctatus* (XP_017327358.1), *Salmo salar* (XP_014035159.1), *Homo sapiens* (NP_001189360.1), *Bos taurus* (NP_776856.1), *Mus musculus* (NP_035164.1), *Rattus norvegicus* (NP_476455.1).

induced *CiPrx1* mRNA highly in different tissues. However, the mRNA level and the time of maximum transcript level varied among them. In liver, the maximum expression *CiPrx1* was observed at 6 h post injection (hpi), in liver and middle kidney, the expression peaks were reached at 12 hpi; while, the greatest transcript level was recorded at 3 hpi in head kidney. After LPS stimulation, the maximum transcript level of *CiPrx1* at 48 hpi in spleen and liver, and the expression was highest at 3 hpi in middle kidney, whereas no significant increase has been found in head kidney.

3.5. Protein expression and western blotting

For better clarifying the function of CiPrx1, the prokaryotic expression experiment was carried out. The CiPrx1 protein was expressed in the pGEX-4T-1 vector in *E. coli* (Transetta DE3) cells. SDS-PAGE analysis showed that recombinant CiPrx1 protein was successfully expressed. The presence of distinct bands corresponding to the fusion protein of expected size, 49.0 kDa (CiPrx1: 22.21 kDa and GST-tag: 26 kDa). The recombinant protein was purified by Glutathione High Capacity Magnetic Agarose Beads according to the manufacturer's instructions (Fig. 7A, line 3). Western blotting of recombinant proteins using the *anti*-GST-tag antibody confirmed a consensus protein 49.0 kDa (Fig. 7B, line 3), which demonstrated that the present results of recombinant expression and purification were successfully performed. This fusion protein was employed to analyze the antioxidant function of CiPrx1 (Fig. 8).

Table 3
Amino acid sequence similarity of CiPrx1 with other species by Geneious.

Percents of similarity

Percents of similarity	1	2	3	4	5	6	7	8	9	10	11	12	13
1. C.carpio_XP_018963467.1		98	99	94	93	95	82.8	82.8	82.8	81	83	83	84
2. C.carpio_XP_018932944.1	98		71.9	67.5	67.5	68.8	61.6	61.6	61.6	60	61.3	61.3	61.3
3. C.idella	99	71.9		92	92	93.5	79.3	79.8	80.8	81.4	82.4	81.4	82.4
4. D.rerio_NP_001013489.2	94	67.5	92		91.5	91	79.8	80.3	81.3	79.9	81.9	79.9	81.4
5. C.harengus_XP_012672962.1	93	67.5	92	91.5		93.5	80.3	80.8	81.8	79.9	81.9	80.9	81.4
6. I.punctatus_XP_017327358.1	95	68.8	93.5	91	93.5		81.8	82.3	83.3	82.4	84.4	83.4	84.4
7. O.kisutch_XP_020309895.1	82.8	61.6	79.3	79.8	80.3	81.8		99	97.5	79.8	81.8	81.3	81.8
8. O.mykiss_XP_021412501.1	82.8	61.6	79.8	80.3	80.8	82.3	99		97.5	80.3	82.8	82.3	82.8
9. S.salar_XP_014035159.1	82.8	61.6	80.8	81.3	81.8	83.3	97.5	97.5		79.8	81.8	81.3	81.8
10.M.musculus_NP_035164.1	81	60	81.4	79.9	79.9	82.4	79.8	80.3	79.8		97	95	95.5
11.R.norvegicus_NP_476455.1	83	61.3	82.4	81.9	81.9	84.4	81.8	82.8	81.8	97		96.5	97.5
12.B.taurus_NP_776856.1	83	61.3	81.4	79.9	80.9	83.4	81.3	82.3	81.3	95	96.5		96.5
13.H.sapiens_NP_001189360.1	84	61.3	82.4	81.4	81.4	84.4	81.8	82.8	81.8	95.5	97.5	96.5	

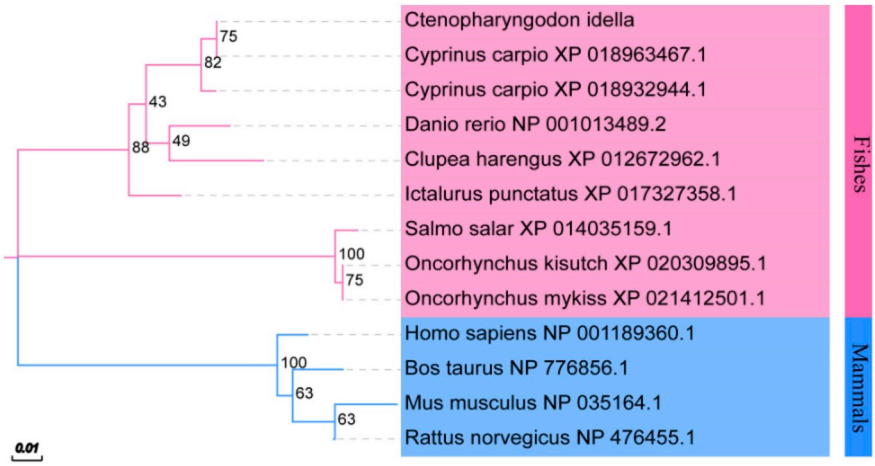

Fig. 3. The neighbor-joining phylogenetic tree analysis of CiPrx1 amino acid sequence with the amino acid sequences of other known Prx1 members; Alignment of amino acid sequences are produced by ClustalW 2.1 and MEGA 5.0. The confidence in each node was assessed by 1000 bootstrap replicates. GenBank accession numbers encoding Prx1 are as follows: *Danio rerio* (NP_001013489.2), *Oncorhynchus kisutch* (XP_020309895.1), *Oncorhynchus mykiss* (XP_021412501.1), *Clupea harengus* (XP_012672962.1), *Cyprinus carpio* (XP_018963467.1, XP_018932944.1), *Ictalurus punctatus* (XP_017327358.1), *Salmo salar* (XP_014035159.1), *Homo sapiens* (NP_001189360.1), *Bos taurus* (NP_776856.1), *Mus musculus* (NP_035164.1), *Rattus norvegicus* (NP_476455.1).

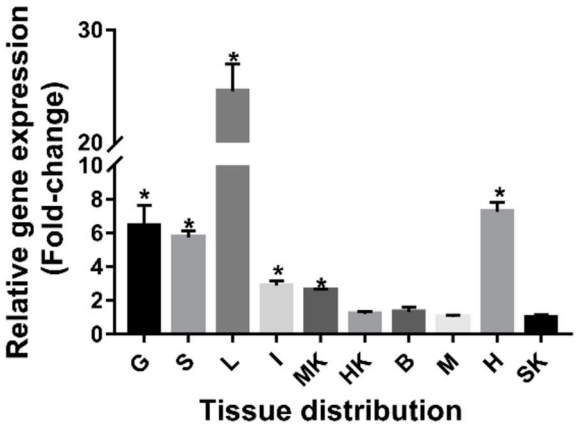

Fig. 4. Expression of *CiPrx1* in different tissues obtained from healthy grass carp. The 10 examined tissues are indicated in abbreviations. SK, skin; G, gill; S, spleen; B, brain; L, liver; HK, head kidney; MK, middle kidney; H, heart; M, muscle; I, intestine. The expression level of *CiPrx1* in skin was set as 1. The β-actin was used as an internal control. The results are presented as the mean ± SD (n = 5). Asterisks (*) representative of significant difference (* = $p \leq 0.05$).

3.6. DNA protection assay through the antioxidant property of CiPrx1

The DNA protection assay was performed to investigate whether the recombinant fusion protein (rCiPrx1) can prevent DNA from damage caused by the ROS generated from the MFO system. In the MFO system, auto-oxidation of thiols like DTT in the presence of metals such as iron generates ROS including, $O_2^{\cdot-}$, ·OH, and H_2O_2. The ·OH radical is able to react with biological molecules, wreaking indiscriminate but extensive intracellular damage. The ROS like ·OH radical, generated nearby the nucleic acids can add hydrogen atoms to DNA bases or abstract hydrogen atoms from the sugar moiety, producing changes like modified bases, DNA strand breaks or abasic sites. The single strand breaks results in the linearization of supercoiled plasmid DNA [(covalently closed circular DNA (CCC DNA)] to open circular plasmid DNA (OC DNA/nicked DNA). The percentage of conversion of CCC DNA to OC DNA suggests the amount of DNA damages caused by ROS and the inhibition of conversion of the CCC DNA to OC DNA, reflects the antioxidant activity of the protein [43]. In this study, pEGFP-N3 plasmid was incubated with rCiPrx1 protein in the MFO system and DNA damage was analyzed by electrophoresis. The MFO system generated using DTT and $FeCl_3$, was able to induce damages to pEGFP-N3 plasmid converting CCC DNA to OC DNA. The results revealed that only $FeCl_3$ affected to damage supercoiled DNA, however, the degree of DNA damage was more serious and DNA was not visible When both DTT and $FeCl_3$ co-existed (Fig. 8, line 2, 4). In addition, the rCiPrx1 protein inhibited DNA damage in a dose-dependent manner compared with the control (Fig. 8). Further, the CiPrx1 protein had the ability to inhibit DNA damage even at lower concentration however protection level increased with the increase of concentration of rCiPrx1 protein.

3.7. Subcellular localization of CiPrx1 in HEK293 cells

To investigate the subcellular localization of the CiPrx1 protein, HEK293 cells were transfected with Prx1-pEGFP plasmids, then fluorescence was observed at 24 h post-transfection. The empty pEGFP-N3 plasmids were also transfected at the same time as the negative control. As shown in Fig. 9, the control pEGFP-N3 was strongly distributed uniformly throughout the entire cell, while Prx1-pEGFP was only strongly distributed in the cytoplasm.

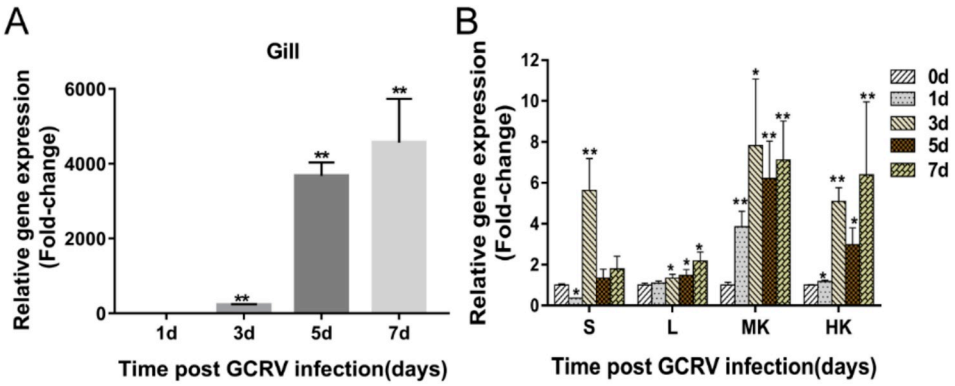

Fig. 5. (A) A relative number of GCRV copies in gill. The relative number of GCRV copies was expressed as the ratio of the level of the S6 segments of GCRV-II expression at different time-point relative to that at 1 dpi. The β-actin was used as an internal control. (B) Expression analysis of *CiPrx1* after GCRV infection. The mRNA expression patterns of *CiPrx1* in fish Spleen (S), Liver (L), Middle kidney (MK) and Head kidney (HK) under GCRV infection were detected by RT-qPCR at 0, 1, 3, 5 and 7 dpi. The β-actin was used as an internal control. The results are presented as the mean ± SD (n = 5). Asterisks (*) representative of significant difference (* = $p \leq 0.05$, ** = $p \leq 0.01$).

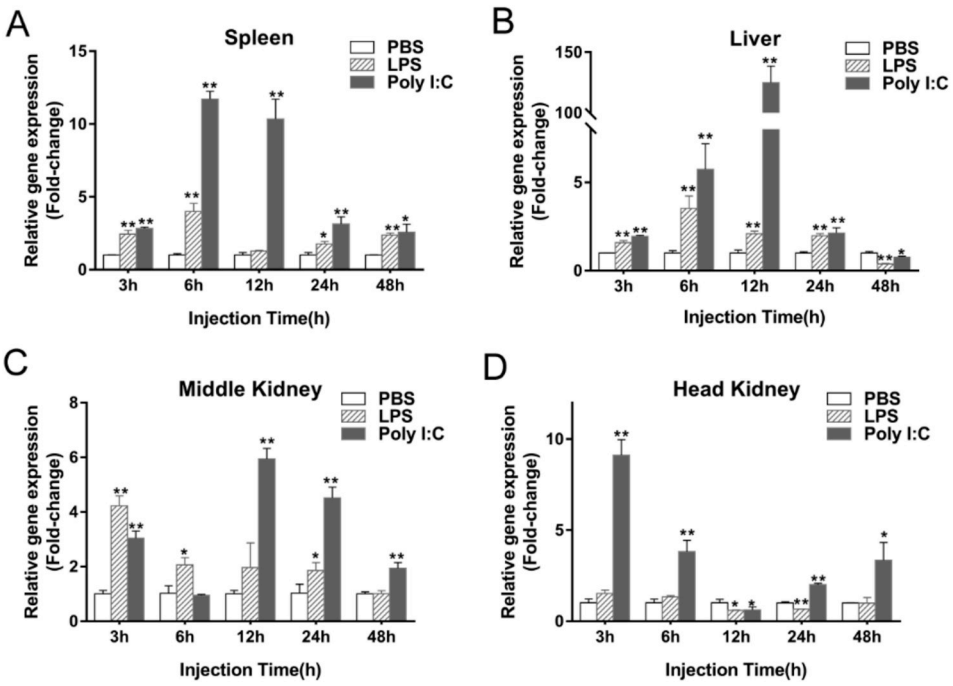

Fig. 6. Expression analysis of *CiPrx1* under stimulation of LPS and Poly I:C. The mRNA expression patterns of *CiPrx1* in fish Spleen (A), Liver (B), Middle kidney (C) and Head kidney (D) under stimulation of LPS and Poly I:C as well as the control group treated with PBS were detected by RT-qPCR at 0, 3, 6, 12, 24 and 48 h post stimulation. The β-actin was used as an internal control. The results are presented as the mean ± SD (n = 5). Asterisks (*) representative of significant difference (* = $p \leq 0.05$, ** = $p \leq 0.01$).

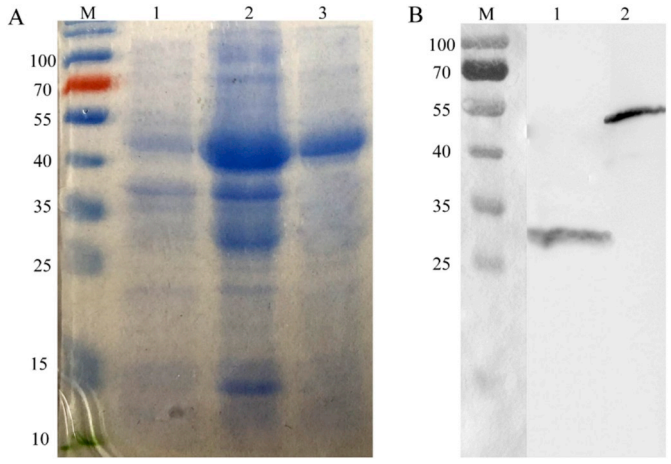

Fig. 7. (A) Sodium dodecyl sulfate-polyacrylamide gel electrophoresis (SDS-PAGE) analysis of CiPrx1 recombinant protein. The gels were visualized by Comassie blue R-250 staining. Lane M: Protein molecular weight marker; Lane 1: before IPTG induction; Lane 2: after 6 h induction with 1.0 mM IPTG; Line 3, Purified recombinant Prx1 protein. (B) Western blot analysis of recombinant proteins in the *E. coli* BL21 (transsetta DE3) cells with *anti*-GST-tag antibody. Lane M: Protein molecular weight marker; Lane 1: GST-tag protein; Lane 2: Purified recombinant CiPrx1 protein. (For interpretation of the references to colour in this figure legend, the reader is referred to the Web version of this article.).

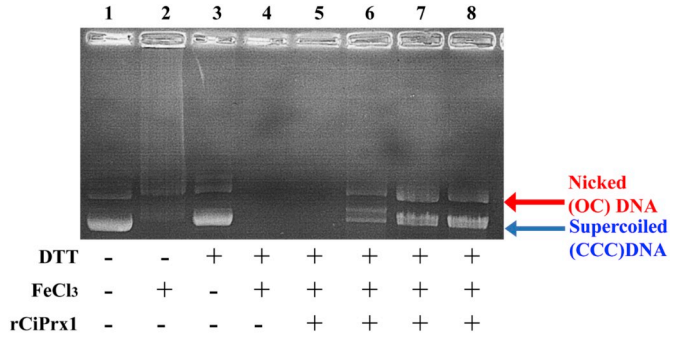

Fig. 8. Protection of supercoiled DNA cleavage by rCiPrx1 in mixed-function oxidase (MFO) assay. 1: pEGFP-N3 without incubation; 2: pEGFP-N3 + $FeCl_3$ (10 μM); 3: pEGFP-N3 + DTT (10 mM); 4: pEGFP-N3 + MFO mix (10 μM $FeCl_3$ + 10 mM DTT); 5: pEGFP-N3 + MFO mix + 1 μg of rCiPrx1; 6: pEGFP-N3 + MFO mix + 5 μg of rCiPrx1; 7: pEGFP-N3 + MFO mix + 20 μg of rCiPrx1; 8: pEGFP-N3 + MFO mix + 30 μg of rCiPrx1. OC DNA: open circular plasmid DNA; CCC: covalently closed circular DNA.

4. Discussion

Prx is a selenium independent peroxidase protein, and it is a large family of antioxidant proteins ubiquitously found in all living organisms from prokaryotes to eukaryotes [44]. In the past decades, Prxs have received increasing attention for their distinctive characteristics in catalytic activity and functioning as chaperonins [22,45,46]. Here, we identified the full-length cDNA sequence of the *CiPrx1* from *C. idella*. The *CiPrx1* gene encodes an approximately 22.21 kDa protein and two highly conserved cysteines (Cys52 and Cys173) were existed in the Prx signature motifs FYPLDFTFVCPTEI and GEVCPA, respectively. The similar results were also found in Prx1 subunits from other species, such as cuttlefish (Cys59 and Cys180) [33], *Lateolabrax japonicas* (Cys51 and Cys172) [34], *Penaeus monodon* (Cys51 and Cys172) [47], golden pompano (Cys51 and Cys172) [36], and Anoplopoma *fimbria* (Cys51 and Cys172) [48], which indicated that *CiPrx1* may have the same antioxidant catalytic attributes as other typical 2-Cys Prxs. The 2-Cys Prxs are divided into two groups, 'typical' and 'atypical' 2-Cys Prxs, depending on whether the conserved cysteine residues form intermolecular or intramolecular disulfide bridges respectively [49]. *CiPrx1* was absent from the signal peptide, which suggests that *CiPrx1* could be secreted like that of human Prx1 via a non-classical ER/Golgi-independent secretory pathway [50]. The deduced amino acid sequence revealed high similarity to previously reported Prx1 from other fishes (80.8–99% sequence similarity). Phylogenetic analysis revealed a closer relationship of *CiPrx1* with other fishes. All these characters indicated that *CiPrx1* were member of typical 2-Cys Prx.

Based on the tissue expression analysis of *CiPrx1*, the *CiPrx1* mRNA was ubiquitously expressed in all tested tissues, although the expression levels varied between tissues, which means that the *CiPrx1* may play a multifunctional role in different tissues of grass carp. Ubiquitous

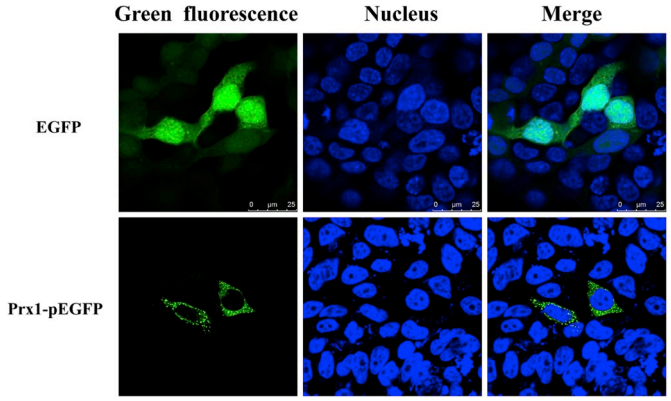

Fig. 9. Subcellular localization of CiPrx1 proteins in HEK 293T cells. HEK 293T cells were plated in 6-well plates. At 24 h post-transfection, cells were fixed with 4% (v/v) paraformaldehyde, permeabilized with 0.2% Triton X-100. Green fluorescence shows the distribution of EGFP or EGFP-tagged proteins, and blue fluorescence shows the nuclei stained with Hoechst 33342 under a 63 × oil immersion objective lens (scale bar, 25 μm). All samples were visualized using a confocal microscope. (For interpretation of the references to colour in this figure legend, the reader is referred to the Web version of this article.).

expression of Prx1 has also been reported in other species [33,34,51]. *SmPrx1* mRNA was highly expressed in the testis, hemocyte, liver, and ovary [33]. The relative high expression levels of *Lateolabrax japonicas Prx1* were detected in the blood, head-kidney and spleen [34]. Cho and his group reported that *Rhodeus uyekii Prx1* mRNA was highly expressed in the intestine, kidney, liver, brain, ovary, and testis, which are involved in the immune response against pathogens [51]. In non-stimulated fish, *CiPrx1* mRNA was highly expressed in the liver and gill. The liver has various functions, including antioxidant activity against metabolic oxidants and detoxification of metabolic by-products or drugs [51]. Meanwhile, high expression level in gill may be due to frequent exposure and high consumption of oxygen, which continuously leads to inducing the production of ROS [52]. The high expressions in immune relevant tissues implied that *CiPrx1* plays important roles in the immune system of grass carp. Therefore, temporal expression of *CiPrx1* post GCRV, LPS and poly(I:C) infection were further analyzed.

Prx1 has been proven that modulates immune response in many species [47,53,54]. After *Lateolabrax japonicas* were treated with different stresses, the *LjPrx1* maximum levels in head kidney were reached at 6 h (*Vibrio harveyi*), 12 h (zinc), 24 h (copper) and 36 h (cadmium and *Streptococcus agalactiae*), However, the expression level of *LjPrx1* peaked in the blood at 12 h (zinc and cadmium), 24 h (*Streptococcus agalactiae*), 36 h (*Vibrio harveyi*) and 48 h (copper) [54]. In *Penaeus monodon, PmPrx1* was clearly upregulated in the hepatopancreas and gills after *Vibrio harveyi* challenge and slightly upregulated after *Streptococcus agalactiae* challenge [47]. After *Vibrio alginolyticus* challenge. The expression of SmPrx1 mRNA was up-regulated in liver and hemocyte [53]. In addition, Prx1 also promotes the cytotoxicity of NK cells against transformed and virus-infected cells [55,56] or regulates the immune reactions by associating with other extracellular factors such as migration inhibitory factor [57]. Our results suggested that *CiPrx1* can be induced by GCRV, LPS and Poly I:C infection in grass carp. Moreover, the *CiPrx1* expression pattern was differently treated with different infectious agents. It may be because the infection of bacterial and viral leads to increased ROS production [12,58,59], and *CiPrx1* was appropriately induced to remove these oxidative stress products.

Prxs are thought to have a role in the inhibition of DNA damage caused by ROS [60]. Our study illustrated the protective role of the rCiPrx1 protein against ROS-mediated DNA damage. Recent studies on *Oplegnathus fasciatus* Prx5 [43], *Procambarus clarkii* Prx5 [61], and *Procambarus clarkii* Prx4 [42] also showed similar results. It further investigating the antioxidant function of Prx1 in teleosts.

Immunohistochemistry staining showed that Prx1 expressed in the cytoplasm of renal tubular epithelial cells, in the kidneys of UUO rats [62]. Fujii et al. found that both Prx1 and Prx2 subcellular localization in the cytoplasm [63]. So, the subcellular localization of CiPrx1 protein in the cytoplasm was also consistent with previous data.

5. Conclusion

In conclusion, we have cloned and characterized an ortholog of Prx1 gene from grass carp for the first time. The *CiPrx1* mRNA was ubiquitously expressed in the examined tissues; further, we observed the up-regulation of *CiPrx1* in the different tissues after GCRV, LPS and Poly I:C infection. Subcellular localization of CiPrx1 was only strongly distributed in the cytoplasm. Moreover, rCiPrx1 protein was found a potential antioxidant enzyme, that could inhibit DNA damage from oxidants. These data together affirm the functional existence of *CiPrx1* in grass carp. Novel functions of Prx1 in teleosts, similar to mammalian Prxs is yet to be investigated. The latter conjecture may be a source for future research in teleosts.

Acknowledgments

Funding: This work was supported by the National Natural Science Foundation of China (grant numbers 31572614 and 31721005).

References

[1] Y. Rao, J. Su, Insights into the antiviral immunity against grass carp (Ctenopharyngodon idella) reovirus (GCRV) in grass carp, J. Immunol. Res. 2015 (2015) 670437.
[2] D. Zhu, R. Huang, L. Chen, P. Fu, L. Luo, L. He, Y. Li, L. Liao, Z. Zhu, Y. Wang, Cloning and characterization of the LEF/TCF gene family in grass carp (Ctenopharyngodon idella) and their expression profiles in response to grass carp reovirus infection, Fish Shellfish Immunol. 86 (2019) 335–346.
[3] L. Chen, R. Huang, D. Zhu, Y. Wang, R. Mehjabin, Y. Li, L. Liao, L. He, Z. Zhu, Y. Wang, Cloning of six serpin genes and their responses to GCRV infection in grass carp (Ctenopharyngodon idella), Fish Shellfish Immunol. 86 (2019) 93–100.
[4] L. Luo, D. Zhu, R. Huang, L. Xiong, R. Mehjabin, L. He, L. Liao, Y. Li, Z. Zhu, Y. Wang, Molecular cloning and preliminary functional analysis of six RING-between-ring (RBR) genes in grass carp (Ctenopharyngodon idellus), Fish Shellfish Immunol. 87 (2019) 62–72.
[5] R. Mehjabin, L. Chen, R. Huang, D. Zhu, C. Yang, Y. Li, L. Liao, L. He, Z. Zhu, Y. Wang, Expression and localization of grass carp pkc-theta (protein kinase C theta) gene after its activation, Fish Shellfish Immunol. 87 (2019) 788–795.
[6] C.M. Fauquet, J. Stanley, Revising the way we conceive and name viruses below the species level: a review of geminivirus taxonomy calls for new standardized isolate descriptors, Arch. Virol. 150 (10) (2005) 2151–2179.
[7] Q. Fang, H. Attoui, J.F.P. Biagini, Z.Y. Zhu, P. de Micco, X. de Lamballerie, Sequence of genome segments 1, 2, and 3 of the grass carp reovirus (genus Aquareovirus, family Reoviridae) (vol 274, pg 762, 2000), Biochem. Biophys. Res. Commun. 276 (1) (2000) 391-391.
[8] M. Korenaga, T. Wang, Y.C. Li, L.A. Showalter, T.S. Chan, J.R. Sun, S.A. Weinman, Hepatitis C virus core protein inhibits mitochondrial electron transport and increases reactive oxygen species (ROS) production, J. Biol. Chem. 280 (45) (2005) 37481–37488.
[9] B. Gruhne, R. Sompallae, D. Marescotti, S.A. Kamranvar, S. Gastaldello, M.G. Masucci, The Epstein-Barr virus nuclear antigen-1 promotes genomic instability via induction of reactive oxygen species, Proc. Natl. Acad. Sci. U.S.A. 106 (7) (2009) 2313–2318.
[10] M.A. Torres, J.D.G. Jones, J.L. Dangl, Reactive oxygen species signaling in response to pathogens, Plant Physiol. 141 (2) (2006) 373–378.
[11] W.H. Tung, H.W. Tsai, I.T. Lee, H.L. Hsieh, W.J. Chen, Y.L. Chen, C.M. Yang, Japanese encephalitis virus induces matrix metalloproteinase-9 in rat brain astrocytes via NF-kappa B signalling dependent on MAPKs and reactive oxygen species, Br. J. Pharmacol. 161 (7) (2010) 1566–1583.
[12] T. Finkel, Signal transduction by reactive oxygen species, JCB (J. Cell Biol.) 194 (1) (2011) 7–15.
[13] M.L. Circu, T.Y. Aw, Reactive oxygen species, cellular redox systems, and apoptosis, Free Radic. Biol. Med. 48 (6) (2010) 749–762.
[14] J.J. Haddad, Antioxidant and prooxidant mechanisms in the regulation of redox(y)-sensitive transcription factors, Cell. Signal. 14 (11) (2002) 879–897.
[15] K. Kannan, S.K. Jain, Oxidative stress and apoptosis, Pathophysiology 7 (3) (2000) 153–163.
[16] R. Edge, T.G. Truscott, Prooxidant and antioxidant reaction mechanisms of carotene and radical interactions with vitamins E and C, Nutrition 13 (11–12) (1997) 992–994.

[17] F. Zhao, Q.H. Wang, The protective effect of peroxiredoxin II on oxidative stress induced apoptosis in pancreatic beta-cells, Cell Biosci. 2 (2012).
[18] C. Bogdan, M. Rollinghoff, A. Diefenbach, Reactive oxygen and reactive nitrogen intermediates in innate and specific immunity, Curr. Opin. Immunol. 12 (1) (2000) 64–76.
[19] G.W. Thorpe, C.S. Fong, N. Alic, V.J. Higgins, I.W. Dawes, Cells have distinct mechanisms to maintain protection against different reactive oxygen species: oxidative-stress-response genes, Proc. Natl. Acad. Sci. U.S.A. 101 (17) (2004) 6564–6569.
[20] C.H. Li, D.J. Ni, L.S. Song, J. Zhao, H. Zhang, L. Li, Molecular cloning and characterization of a catalase gene from Zhikong scallop Chlamys farreri, Fish Shellfish Immunol. 24 (1) (2008) 26–34.
[21] S.G. Rhee, H.Z. Chae, K. Kim, Peroxiredoxins: a historical overview and speculative preview of novel mechanisms and emerging concepts in cell signaling, Free Radic. Biol. Med. 38 (12) (2005) 1543–1552.
[22] K. Kim, I.H. Kim, K.Y. Lee, S.G. Rhee, E.R. Stadtman, The isolation and purification of a specific "protector" protein which inhibits enzyme inactivation by a thiol/Fe (III)/O2 mixed-function oxidation system, J. Biol. Chem. 263 (10) (1988) 4704–4711.
[23] K. Kim, S.G. Rhee, E.R. Stadtman, Nonenzymatic cleavage of proteins by reactive oxygen species generated by dithiothreitol and iron, J. Biol. Chem. 260 (29) (1985) 5394–5397.
[24] M.R. Si, T.T. Wang, J.F. Pan, J.S. Lin, C. Chen, Y.H. Wei, Z.Q. Lu, G.H. Wei, X.H. Shen, Graded response of the multifunctional 2-cysteine peroxiredoxin, CgPrx, to increasing levels of hydrogen peroxide in corynebacterium glutamicum, Antioxidants Redox Signal. 26 (1) (2017) 1–14.
[25] H.H. Jang, K.O. Lee, Y.H. Chi, B.G. Jung, S.K. Park, J.H. Park, J.R. Lee, S.S. Lee, J.C. Moon, J.W. Yun, Y.O. Choi, W.Y. Kim, J.S. Kang, G.W. Cheong, D.J. Yun, S.G. Rhee, M.J. Cho, S.Y. Lee, Two enzymes in one: two yeast peroxiredoxins display oxidative stress-dependent switching from a peroxidase to a molecular chaperone function, Cell 117 (5) (2004) 625–635.
[26] A. Matte, L. De Falco, A. Iolascon, N. Mohandas, X.L. An, A. Siciliano, C. Leboeuf, A. Janin, M. Bruno, S.Y. Choi, D.W. Kim, L. De Franceschi, The interplay between peroxiredoxin-2 and nuclear factor-erythroid 2 is important in limiting oxidative mediated dysfunction in beta-thalassemic erythropoiesis, Antioxidants Redox Signal. 23 (16) (2015) 1284–1297.
[27] M. Olahova, S.R. Taylor, S. Khazaipoul, J.L. Wang, B.A. Morgan, K. Matsumoto, T.K. Blackwell, E.A. Veal, A redox-sensitive peroxiredoxin that is important for longevity has tissue- and stress-specific roles in stress resistance, Proc. Natl. Acad. Sci. U.S.A. 105 (50) (2008) 19839–19844.
[28] S.G. Rhee, H.A. Woo, Multiple functions of peroxiredoxins: peroxidases, sensors and regulators of the intracellular messenger H2O2, and protein chaperones, Antioxidants Redox Signal. 15 (3) (2011) 781–794.
[29] H.A. Woo, S.H. Yim, D.H. Shin, D. Kang, D.Y. Yu, S.G. Rhee, Inactivation of peroxiredoxin I by phosphorylation allows localized H2O2 accumulation for cell signaling, Cell 140 (4) (2010) 517–528.
[30] Z.A. Wood, L.B. Poole, P.A. Karplus, Peroxiredoxin evolution and the regulation of hydrogen peroxide signaling, Science 300 (5619) (2003) 650–653.
[31] T. Nystrom, J.S. Yang, M. Molin, Peroxiredoxins, gerontogenes linking aging to genome instability and cancer, Genes Dev. 26 (18) (2012) 2001–2008.
[32] N. Wijayanti, S. Naidu, T. Kietzmann, S. Immenschuh, Inhibition of phorbol ester-dependent peroxiredoxin I gene activation by lipopolysaccharide via phosphorylation of Re1A/p65 at serine 276 in monocytes, Free Radic. Biol. Med. 44 (4) (2008) 699–710.
[33] W.W. Song, C.K. Mu, R.H. Li, C.L. Wang, Peroxiredoxin 1 from cuttlefish (Sepiella maindroni): molecular characterization of development and its immune response against Vibrio alginolyticus, Fish Shellfish Immunol. 67 (2017) 596–603.
[34] K.F. Xu, G.D. Wang, Identification and characterization of peroxiredoxin 1 from Lateolabrax japonicus under biotic and abiotic stresses, Fish Shellfish Immunol. 81 (2018) 297–303.
[35] Z. Hu, K.S. Lee, Y.M. Choo, H.J. Yoon, S.M. Lee, J.H. Lee, D.H. Kim, H.D. Sohn, B.R. Jin, Molecular cloning and characterization of 1-Cys and 2-Cys peroxiredoxins from the bumblebee Bombus ignitus, Comp. Biochem. Physiol. B 155 (3) (2010) 272–280.
[36] L. Wang, H.Y. Guo, N. Zhang, Z.H. Ma, S.G. Jiang, D.C. Zhang, Molecular characterization and functional analysis of a peroxiredoxin 1 cDNA from golden pompano (Trachinotus ovatus), Dev. Comp. Immunol. 51 (2) (2015) 261–270.
[37] J. Van Horn, V. Malhoe, M. Delvina, M. Thies, S.G. Tolley, T. Ueda, Molecular cloning and expression of a 2-Cys peroxiredoxin gene in the crustacean Eurypanopeus depressus induced by acute hypo-osmotic stress, Comp. Biochem. Physiol. B 155 (3) (2010) 309–315.
[38] D. Zhu, R. Huang, P. Fu, L. Chen, L. Luo, P. Chu, L. He, Y. Li, L. Liao, Z. Zhu, Y. Wang, Investigating the role of BATF3 in grass carp (Ctenopharyngodon idella) immune modulation: a fundamental functional analysis, Int. J. Mol. Sci. 20 (7) (2019) 1687.
[39] Y. Wang, Y. Lu, Y. Zhang, Z. Ning, Y. Li, Q. Zhao, H. Lu, R. Huang, X. Xia, Q. Feng, X. Liang, K. Liu, L. Zhang, T. Lu, T. Huang, D. Fan, Q. Weng, C. Zhu, Y. Lu, W. Li, Z. Wen, C. Zhou, Q. Tian, X. Kang, M. Shi, W. Zhang, S. Jang, F. Du, S. He, L. Liao, Y. Li, B. Gui, H. He, Z. Ning, C. Yang, L. He, L. Luo, R. Yang, Q. Luo, X. Liu, S. Li, W. Huang, L. Xiao, H. Lin, B. Han, Z. Zhu, The draft genome of the grass carp (Ctenopharyngodon idellus) provides insights into its evolution and vegetarian adaptation, Nat. Genet. 47 (6) (2015) 625–631.
[40] N. Saitou, M. Nei, The neighbor-joining method: a new method for reconstructing phylogenetic trees, Mol. Biol. Evol. 4 (4) (1987) 406–425.
[41] K.J. Livak, T.D. Schmittgen, Analysis of relative gene expression data using real-time quantitative PCR and the 2(T)(-Delta Delta C) method, Methods 25 (4) (2001) 402–408.
[42] L.-S. Dai, X.-M. Yu, M.N. Abbas, C.-S. Li, S.-H. Chu, S. Kausar, T.-T. Wang, Essential role of the peroxiredoxin 4 in Procambarus clarkii antioxidant defense and immune responses, Fish Shellfish Immunol. 75 (2018) 216–222.
[43] K. Saranya Revathy, N. Umasuthan, I. Whang, H.B. Jung, B.S. Lim, B.H. Nam, J. Lee, A potential antioxidant enzyme belonging to the atypical 2-Cys peroxiredoxin subfamily characterized from rock bream, Oplegnathus fasciatus, Comp. Biochem. Physiol. B Biochem. Mol. Biol. 187 (2015) 1–13.
[44] H.Z. Chae, S.J. Chung, S.G. Rhee, Thioredoxin-dependent peroxide reductase from yeast, J. Biol. Chem. 269 (44) (1994) 27670–27678.
[45] H.H. Jang, K.O. Lee, Y.H. Chi, B.G. Jung, S.K. Park, J.H. Park, J.R. Lee, S.S. Lee, J.C. Moon, J.W. Yun, Y.O. Choi, W.Y. Kim, J.S. Kang, G.W. Cheong, D.J. Yun, S.G. Rhee, M.J. Cho, S.Y. Lee, Two enzymes in one; two yeast peroxiredoxins display oxidative stress-dependent switching from a peroxidase to a molecular chaperone function, Cell 117 (5) (2004) 625–635.
[46] R.S. Edgar, E.W. Green, Y. Zhao, G. van Ooijen, M. Olmedo, X. Qin, Y. Xu, M. Pan, U.K. Valekunja, K.A. Feeney, E.S. Maywood, M.H. Hastings, N.S. Baliga, M. Merrow, A.J. Millar, C.H. Johnson, C.P. Kyriacou, J.S. O'Neill, A.B. Reddy, Peroxiredoxins are conserved markers of circadian rhythms, Nature 485 (7399) (2012) 459–464.
[47] R. Bu, P. Wang, C. Zhao, W. Bao, L. Qiu, Gene characteristics, immune and stress responses of PmPrx1 in black tiger shrimp (Penaeus monodon): insights from exposure to pathogenic bacteria and toxic environmental stressors, Dev. Comp. Immunol. 77 (2017) 1–16.
[48] J. Konig, K. Lotte, R. Plessow, A. Brockhinke, M. Baier, K.J. Dietz, Reaction mechanism of plant 2-Cys peroxiredoxin. Role of the C terminus and the quaternary structure, J. Biol. Chem. 278 (27) (2003) 24409–24420.
[49] Z.A. Wood, E. Schroder, J.R. Harris, L.B. Poole, Structure, mechanism and regulation of peroxiredoxins, Trends Biochem. Sci. 28 (1) (2003) 32–40.
[50] Y. Chen, Y.-X. Zhang, T.-J. Fan, L. Meng, G.-c. Ren, S.-L. Chen, Molecular identification and expression analysis of the natural killer cell enhancing factor (NKEF) gene from turbot (Scophthalmus maximus), Aquaculture 261 (4) (2006) 1186–1193.
[51] H.K. Cho, H.J. Kong, J.Y. Moon, J.D. Kim, D.G. Kim, W.J. Kim, B.H. Nam, Y.O. Kim, H.S. Kim, C.M. An, B.S. Kim, Molecular characterization and expression analysis of a peroxiredoxin 1 cDNA from Korean rose bitterling (Rhodeus uyekii), Mol. Biol. Rep. 41 (4) (2014) 2363–2370.
[52] W.A. Pushpamali, M. De Zoysa, H.S. Kang, C.H. Oh, I. Whang, S.J. Kim, J. Lee, Comparative study of two thioredoxin peroxidases from disk abalone (Haliotis discus discus): cloning, recombinant protein purification, characterization of antioxidant activities and expression analysis, Fish Shellfish Immunol. 24 (3) (2008) 294–307.
[53] W. Song, C. Mu, R. Li, C. Wang, Peroxiredoxin 1 from cuttlefish (Sepiella maindroni): molecular characterization of development and its immune response against Vibrio alginolyticus, Fish Shellfish Immunol. 67 (2017) 596–603.
[54] K. Xu, G. Wang, Identification and characterization of peroxiredoxin 1 from Lateolabrax japonicus under biotic and abiotic stresses, Fish Shellfish Immunol. 81 (2018) 297–303.
[55] R. Geiben-Lynn, M. Kursar, N.V. Brown, M.M. Addo, H. Shau, J. Lieberman, A.D. Luster, B.D. Walker, HIV-1 antiviral activity of recombinant natural killer cell enhancing factors, NKEF-A and NKEF-B, members of the peroxiredoxin family, J. Biol. Chem. 278 (3) (2003) 1569–1574.
[56] H. Sauri, P.H. Ashjian, A.T. Kim, H. Shau, Recombinant natural killer enhancing factor augments natural killer cytotoxicity, J. Leukoc. Biol. 59 (6) (1996) 925–931.
[57] H. Jung, T. Kim, H.Z. Chae, K.T. Kim, H. Ha, Regulation of macrophage migration inhibitory factor and thiol-specific antioxidant protein PAG by direct interaction, J. Biol. Chem. 276 (18) (2001) 15504–15510.
[58] Y. Duan, J. Zhang, H. Dong, Y. Wang, Q. Liu, H. Li, Oxidative Stress Response of the Black Tiger Shrimp Penaeus monodon to Vibrio Parahaemolyticus Challenge, (2015).
[59] K. Junkunlo, K. Soderhall, I. Soderhall, C. Noonin, Reactive oxygen species affect transglutaminase activity and regulate hematopoiesis in a Crustacean, J. Biol. Chem. 291 (34) (2016) 17593–17601.
[60] C.A. Neumann, D.S. Krause, C.V. Carman, S. Das, D.P. Dubey, J.L. Abraham, R.T. Bronson, Y. Fujiwara, S.H. Orkin, R.A. Van Etten, Essential role for the peroxiredoxin Prdx1 in erythrocyte antioxidant defence and tumour suppression, Nature 424 (6948) (2003) 561–565.
[61] L. Wu, Y. Zhou, M.N. Abbas, S. Kausar, Q. Chen, C.-X. Jiang, L.-S. Dai, Molecular structure and functional characterization of the peroxiredoxin 5 in Procambarus clarkii following LPS and Poly I:C challenge, Fish Shellfish Immunol. 71 (2017) 28–34.
[62] W. Mei, Z. Peng, M. Lu, C. Liu, Z. Deng, Y. Xiao, J. Liu, Y. He, Q. Yuan, X. Yuan, D. Tang, H. Yang, L. Tao, Peroxiredoxin 1 inhibits the oxidative stress induced apoptosis in renal tubulointerstitial fibrosis, Nephrology 20 (11) (2015) 832–842.
[63] J. Fujii, Y. Ikeda, Advances in our understanding of peroxiredoxin, a multifunctional, mammalian redox protein, Redox Rep. 7 (3) (2002) 123–130.